A theoretical model to describe the influence of material microstructure on fatigue crack propagation

Roberto Brighenti[1,a] , Andrea Carpinteri[1,b] , Andrea Spagnoli[1,c]

[1] Department of Civil-Environmental Engineering & Architecture, University of Parma

Viale G.P. Usberti 181/A, 43124 Parma, Italy

[a] brigh@unipr.it, [b] andrea.carpinteri@unipr.it, [c] spagnoli@unipr.it

Abstract. The evaluation of crack initiation, short crack growth as well as crack path at microscopic scale are crucial issues for the safety assessment of macroscopically fracture-free structural components. In the present paper, the crack propagation at the material microscale is modelled by taking into account the spatial variability of mechanical characteristics of the material as well as the local multiaxial stress field disturbance induced by properly-defined equivalent inclusions. By adopting some crack extension criteria under mixed mode, the short crack path is determined. A strong microstructure dependence of the crack path arises in the short-crack regime, while the microstructure of the material does not influence the crack propagation for sufficiently long cracks. An average equivalent SIF is computed for kinked short cracks, and a law to estimate the fatigue crack growth rate is proposed.

Introduction

The evaluation of fatigue crack growth at small scale, that is, when the crack size is comparable with a characteristic length of the material (e.g. grain size in metallic materials), is still an open problem. In this context, the crack propagation in a inhomogeneous material is assumed to depend on the mechanical barriers to the crack growth produced by the microstructure. Moreover, the plastic zone size at crack tip at small scale is comparable with the crack size, leading to the violation of the small-scale yielding hypothesis. A simple way to take into account the effects of the material microstructure on the crack growth at small scale [1] consists in using the non-uniform stress field induced by embedded inohomogeneities: in fact, even for a uniform remote stress applied to the structural component, an oscillating stress field might develop at the microscale.

In the present paper, by superimposing the solution of a homogeneous elastic infinite plate to that of a circular elastic inclusion, the stress field in the case of several non-interacting inclusions is determined, and the corresponding mixed mode Stress Intensity Factors (SIFs) are computed. Crack paths under static loading are evaluated by applying both the maximum principal stress criterion [2, 3] and the minimum plastic zone extension criterion (R-criterion, [4, 5]). The trajectory described by the crack tip is deduced through an incremental method, where the Mode I and Mode II SIFs of the kinked crack are approximately evaluated as a function of the SIFs related to a projected straight crack. An equivalent mean weighted Mode I SIF (useful for fatigue crack assessment) in such cases is also determined. Finally, some examples related to metallic alloys are examined. It is shown that small-scale fluctuations of the stress field heavily affect the crack paths for short cracks, while such an influence disappears for sufficiently long cracks after reaching a transition point during the crack propagation process. Further, the equivalent SIF is strongly affected by the material microstructure for short cracks, while it tends to the case of homogeneous materials for long cracks.

Stress Field at the Microscale due to Material Inhomogeneities

Structural materials are always characterized by heterogeneities at the mesoscale or microscale, due to either the multiphase nature of the materials (such as for composite materials) or unavoidable inhomogeneities (such as in metallic alloys composed by a base material and secondary inclusions). Because of the above heterogeneous microstructure, the stress field at such a scale might be non-uniform and multiaxial even if a uniaxial uniform remote stress is applied.
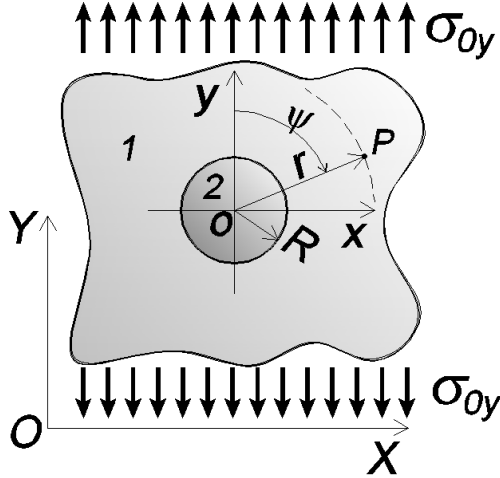
Fig. 1. Circular elastic inclusion in an infinite elastic plate under remote uniform tensile stress σ_{0y}.

It is worth noting that a local fluctuation of the microstress field can heavily influence the crack paths for flaws with length comparable to the characteristic material length.

The modelling rationale here adopted to describe the inhomogeneities contained in the material is based on a periodic distribution of spherical particles embedded in the base material.

By considering a single inclusion (material 2) of radius R embedded in an infinite plate (material 1) under remote uniform stress (Fig. 1), the elastic stress field can be determined by applying the superposition principle together with the Kirsch solution [6]. The resulting stress field, $\bar{\sigma}_x$, $\bar{\sigma}_y$, $\bar{\tau}_{xy}$, is uniform within the inclusion, and can be expressed through the remote stress σ_{0y} as follows:

$$\bar{\sigma}_x = k_x \cdot \sigma_{0y}, \quad \bar{\sigma}_y = k_y \cdot \sigma_{0y}, \quad \bar{\tau}_{xy} = 0 \tag{1}$$

By assuming the x-y coordinate system origin in the inclusion centre (Fig. 1), the stress field components $\sigma_x, \sigma_y, \tau_{xy}$ in the region around the inclusion (point P in Fig. 1) can be expressed as follows under plane stress condition [6]:

$$\sigma_x = \sigma_{0y} \cdot \left[\frac{(1-k_y+k_x)R^2}{2r^2} \cdot \left(3 - \frac{3R^2+18y^2}{r^2} + F - G \right) + \frac{k_x R^2}{r^2}\left(1 - \frac{2y^2}{r^2}\right) \right]$$

$$\sigma_y = \sigma_{0y} \cdot \left[1 + \frac{(1-k_y+k_x)R^2}{2r^2} \cdot \left(1 + \frac{3R^2+10y^2}{r^2} - F + G \right) - \frac{k_x R^2}{r^2}\left(1 - \frac{2y^2}{r^2}\right) \right] \quad \text{with} \quad r = \sqrt{x^2+y^2} \tag{2}$$

$$\tau_{xy} = \sigma_{0y} \cdot \left[\frac{(1-k_y+k_x)R^2 xy}{r^4} \cdot \left(3 - \frac{6R^2+8y^2}{r^2} + \frac{12R^2 y^2}{r^4} \right) + \frac{2k_x R^2 xy}{r^4} \right]$$

where the coefficients k_x, k_y can be obtained from the knowledge of the elastic constants of the base material (E_1, ν_1) and of the inclusion (E_2, ν_2) (by setting $c = 1 - \nu_1^2$, $F = 8y^2(3R^2+2y^2)/r^4$ and $G = 24R^2 y^4/r^6$) [6]:

$$k_x = \frac{c \cdot E_2\left[(3\nu_2-1)E_1 + (1-3\nu_1)E_2\right]}{E_2^2(8c^2+2c\nu_1-6c+1-\nu_1^2) + E_1^2(1-\nu_2^2) + E_1 E_2(2\nu_1\nu_2-2+6c-2c\nu_2)}$$

$$\tag{3}$$

$$k_y = \frac{c \cdot E_2\left[E_1(3-\nu_2) + E_2(8c-3+\nu_1)\right]}{E_2^2(8c^2+2c\nu_1-6c+1-\nu_1^2) + E_1^2(1-\nu_2^2) + E_1 E_2(2\nu_1\nu_2-2+6c-2c\nu_2)}$$

The elastic stress field in such heterogeneous materials can be approximately computed by using the
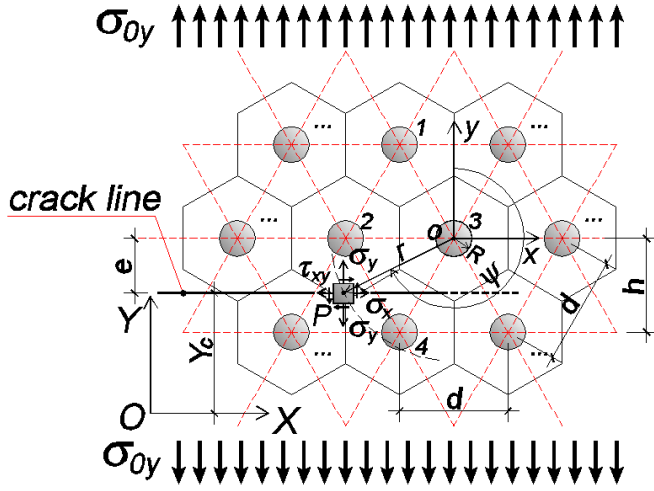
Fig. 2. Equally-spaced circular inclusions in an infinite domain arranged in a hexagonal cell pattern having characteristic size d, under remote uniform tensile stress σ_{0y}.

single inclusion solution and the superposition principle, provided that the inclusions are assumed to be non-interacting (as reasonably occuring for widely spaced inclusions).

By considering point P belonging to the base material (Fig. 2), the resulting stress field is approximately determined by summing up the effects of the inclusions (such as particles 1, 2, 3, 4, etc., Fig. 2):

$$\sigma_x(P) = \sum_i \sigma_{(i)x}(r_{(i)P}, \theta_{(i)P})$$
$$\sigma_y(P) = \sigma_{0y} + \sum_i \left[\sigma_{(i)y}(r_{(i)P}, \theta_{(i)P}) - \sigma_{0y} \right]$$
$$\tau_{xy}(P) = \sum_i \tau_{(i)xy}(r_{(i)P}, \theta_{(i)P}) \qquad (4)$$

where the cartesian stress components

$\sigma_{(i)x}(r_{(i)P}, \theta_{(i)P})$, $(\sigma_{(i)y}(r_{(i)P}, \theta_{(i)P}) - \sigma_{0y})$, $\tau_{(i)xy}(r_{(i)P}, \theta_{(i)P})$ indicate the stress fluctuations evaluated in P in an elastic infinite plate containing a single inclusion i ($i = 1,2,3,4,.....$), under the remote stress σ_{0y}. The summation in Eq. (4) must be performed by taking into account all the inclusions that are within a significant *influence region* around the point P under consideration, and neglecting the inclusions at a large distance from P. Figure 3 shows the stress fluctuations along different lines and for regular hexagonal lattice arrangement of particles.
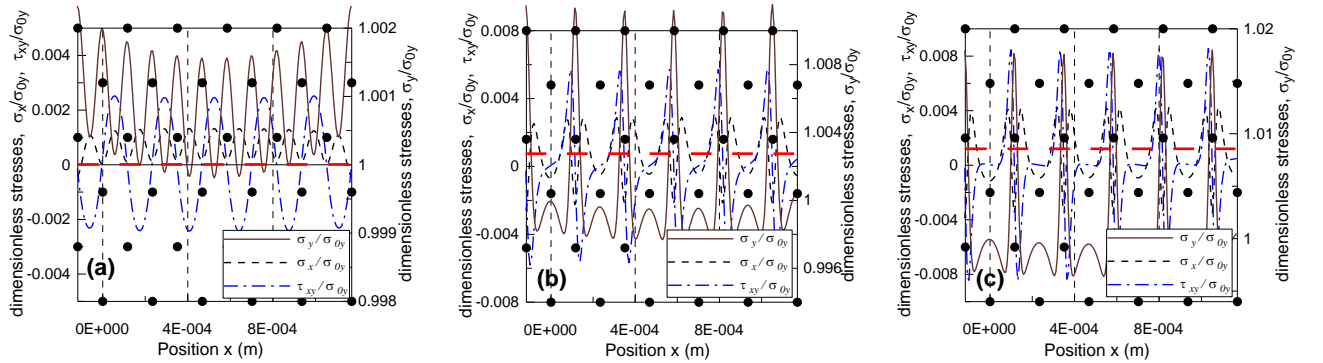
Fig. 3. Dimensionless stresses along a horizontal straight path (dashed line) located at (a) e/h=1/2, (b) e/h=1/4 and (c) e/h=1/5 distance between two lines of inclusions ($d = 2.34 \cdot 10^{-4}$ m), in an infinite plate under remote tensile stress σ_{0y}. Dots indicate the positions of inclusions in the material.

Approximate SIFs in Nominally-Mode I Kinked Crack

The SIF of a straight crack (in an infinite plate) with length 2l, normal to the uniform remote stress σ_{0y} direction, is $K_I^{(\infty)} = \sigma_{0y}\sqrt{\pi l}$. A generic stress influenced by the inclusions (Eqs 2-4) can be decomposed in a remote uniform uniaxial stress σ_{0y} and a fluctuating multiaxial stress field $\tilde{\mathbf{T}}(x)$ here assumed to be a one-dimensional function of the x coordinate. The stress field given by $\tilde{\mathbf{T}}(x)$ is a self-balanced microstress field, characterized by a material length d (inclusion spacing), with

two non-zero stress components $\tilde{\sigma}_y = \tilde{\sigma} = f(x/d)\tilde{\sigma}_a$ and $\tilde{\tau}_{xy} = \tilde{\tau} = f(x/d)\tilde{\tau}_a$, whereas $\tilde{\sigma}_x$ is assumed to be negligible. For the sake of simplicity, we assume the function $f(x/d)$ to be approximate through a Fourier series, i.e. $f(x/d) = \cos(2\pi x/d)$ (Fig. 4a). Under the self-balanced microstresses $\tilde{\sigma}$ and $\tilde{\tau}$, the SIFs (of the projected crack) are computed using the superposition principle:

$$\tilde{K}_I = 2\sqrt{\frac{l}{\pi}}\int_0^l \frac{\tilde{\sigma}}{\sqrt{l^2-x^2}}dx = 2\tilde{\sigma}_a\sqrt{\frac{l}{\pi}}\int_0^l \frac{f(x/d)}{\sqrt{l^2-x^2}}dx = 2\tilde{\sigma}_a\sqrt{\frac{l}{\pi}}\int_0^l \frac{\cos(2\pi x/d)}{\sqrt{l^2-x^2}}dx = \tilde{\sigma}_a\sqrt{\pi l}J_0\left(\frac{2\pi l}{d}\right)$$

$$\tilde{K}_{II} = 2\sqrt{\frac{l}{\pi}}\int_0^l \frac{\tilde{\tau}}{\sqrt{l^2-x^2}}dx = 2\tilde{\tau}_a\sqrt{\frac{l}{\pi}}\int_0^l \frac{f(x/d)}{\sqrt{l^2-x^2}}dx = 2\tilde{\tau}_a\sqrt{\frac{l}{\pi}}\int_0^l \frac{\cos(2\pi x/d)}{\sqrt{l^2-x^2}}dx = \tilde{\tau}_a\sqrt{\pi l}J_0\left(\frac{2\pi l}{d}\right)$$

(5)

where J_0 is the zero-order Bessel function [7].
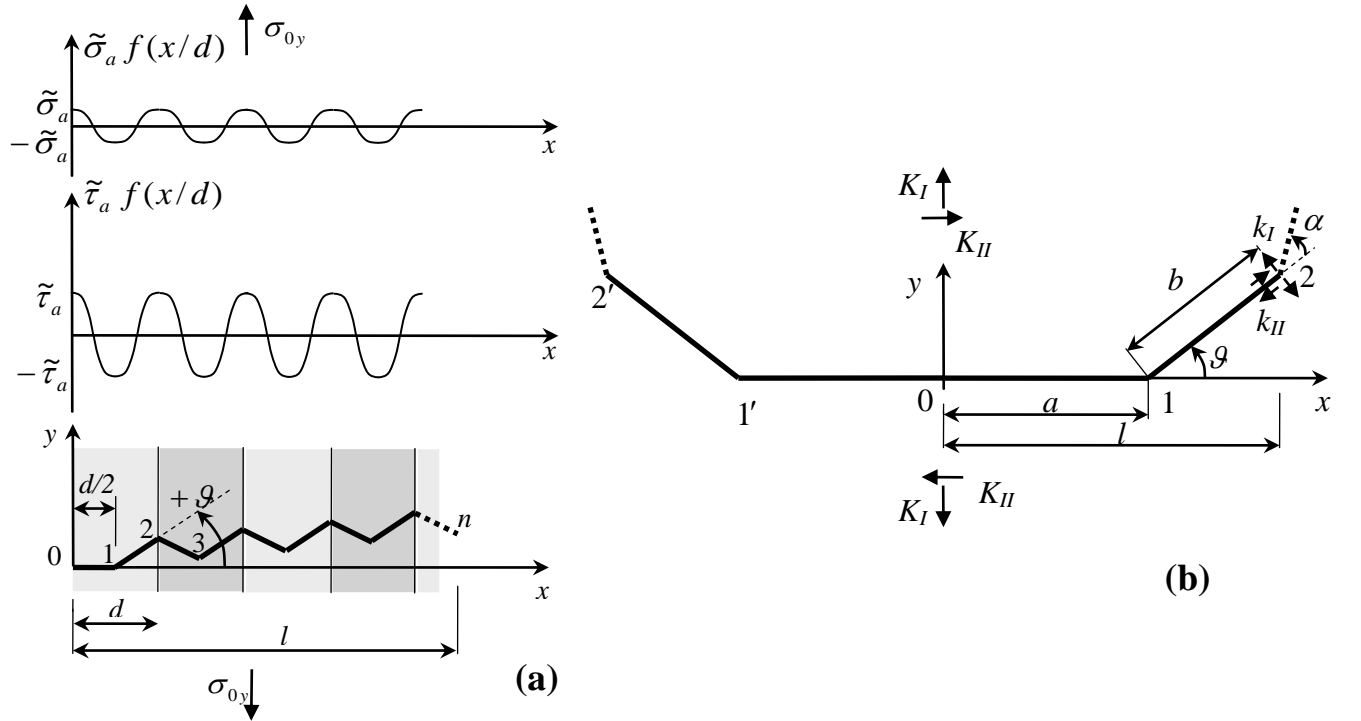
Fig. 4. Self-balanced microstresses (a) and periodically kinked crack in an infinite plate (b).

In LEFM, the total SIFs are simply the sums of the two contributions due to the remote and microstress fields, that is:

$$K_I = K_I^{(\infty)} + \tilde{K}_I, \qquad K_{II} = K_{II}^{(\infty)} + \tilde{K}_{II}$$

(6)

In such a self-balanced microstress field, it can be reasonably assumed that the crack kinks (due to the mixed mode of fracture) symmetrically with respect to the Y-axis and at each material microstructure semi-period, i.e. at each reversal in the microstress spatial courses. In the case of a singly-kinked crack (of projected crack length $2l$), the SIFs at the tips of the inclined part of the crack can be expressed through the SIFs K_I and K_{II} of a straight crack of length equal to the projected length of the kinked crack [8, 9]:

$$k_I = a_{11}(\vartheta, b/a)K_I + a_{12}(\vartheta, b/a)K_{II} \qquad k_{II} = a_{21}(\vartheta, b/a)K_I + a_{22}(\vartheta, b/a)K_{II}$$

(7)

where a_{ij} are coefficients depending on the slant angle ϑ (positive counter-clockwise for tip coordinate x > 0) and the length ratio b/a between the deflected leading segment and the horizontal trailing (preceding) segment (Fig. 4b). For other geometries, the SIFs defined with respect to the projected crack would change, but not the expressions in Eq. (7).

The coefficients a_{ij} for $b/a \to \infty$ (and, with good approximation, also for $b/a > 0.3$) are [8]:

$$a_{11}(\vartheta) = \cos^{3/2} \vartheta, \quad a_{12}(\vartheta) = -2\sin \vartheta \cos^{1/2} \vartheta, \quad a_{21}(\vartheta) = \sin \vartheta \cos^{1/2} \vartheta, \quad a_{22}(\vartheta) = \cos 2\vartheta \cos^{-1/2} \vartheta \qquad (8)$$

Note that the local SIFs in Eqs 7 and 8 are equal to those of an inclined straight crack of projected semi-length l forming an angle $\pi/2 - \vartheta$ with respect to the loading axis [8] (Fig. 5).
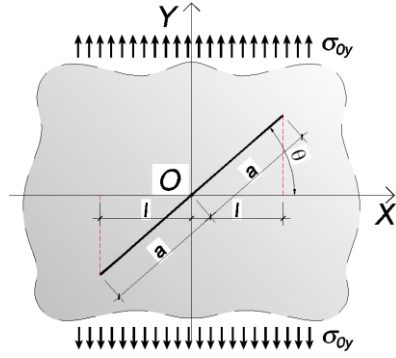
Fig. 5. Infinite cracked plate with an inclined crack under remote tension σ_{0y}.

It can be reasonably assumed that, as the crack propagates following the path in Fig. 4a, only its latter deflection influences the stress field near the crack tips (for example, along the straight segment 2-3 in Fig. 4a, the deflection point 2 has an effect, while the deflection point 1 does not have). The local SIFs at the crack tip are assumed to be expressed by Eqs 7 and 8 for deflected (Mode I+II) segments (see the segments 1-2 and $1' - 2'$ in Fig. 4b).

The approximate computation is thus based on the assumption that the near-tip stress field depends on the local crack direction at the crack tip.

Weighted Average SIF for Nominally-Mode I Kinked Crack

By means of the local Mode I and Mode II SIFs, an equivalent Mode I SIF k_{eq} can be defined through energetic considerations [3], namely:

$$k_{eq} = \sqrt{k_I^2 + k_{II}^2} \qquad (9)$$

and, after substituting Eqs (7, 8) in Eq. (9), we get:

$$k_{eq} = \sqrt{K_I^2 \cos \vartheta + K_{II}^2 \left(4\sin^2 \vartheta \cos \vartheta + \frac{\cos^2 2\vartheta}{\cos \vartheta}\right) + K_I K_{II} \sin \vartheta \left(2\cos 2\vartheta - 4\cos^2 \vartheta\right)} \qquad (10)$$

For a nominally Mode I crack (submitted to a remote Mode I loading) in an infinite plate under constant amplitude cyclic loading, by exploiting the superposition principle, the SIF ranges related to the projected crack of semi-length l, can be written as follows [7]:

$$\Delta K_I = \Delta\sigma^{(\infty)} \sqrt{\pi l}\left[1 + \frac{\Delta\tilde{\sigma}_a}{\Delta\sigma^{(\infty)}} J_0\left(\frac{2\pi l}{d}\right)\right], \quad \Delta K_{II} = \Delta\sigma^{(\infty)} \sqrt{\pi l}\left[\frac{\Delta\tilde{\tau}_a}{\Delta\sigma^{(\infty)}} J_0\left(\frac{2\pi l}{d}\right)\right] \qquad (11)$$

where the microstress field is assumed to vary in time proportionally to the remote stress.

Under remote Mode I loading and local shear microstress field, cracks "on average" propagate normal to the loading axis, following a zig-zag pattern. It can be easily shown that the crack slanting angle, $\vartheta = \vartheta(l/d)$, decreases as the crack length increases with respect to the material microstructural length d.

A mean weighted value $\Delta\overline{K}_{I,eq}$ of the equivalent SIF range Δk_{eq} along the straight segments (the crack path is assumed to be a repetitive pattern constituted by n segments) is defined as follows:

$$\Delta\overline{K}_{I,eq}(s_n) = \left(\sum_{i=1}^{n}(s_i - s_{i-1})\Delta k_{eq,i}\right)/s_n \qquad (12)$$

where $\Delta k_{eq,i}$ (Eq. 10) is the equivalent SIF value along the straight segment of length $(s_i - s_{i-1})$, s being the curvilinear coordinate along the crack path. In the particular case of ϑ constant we get:

$$\Delta \overline{K}_{I,eq} = \Delta k_{eq} = \sqrt{\Delta K_I^2 \cos \vartheta + \Delta K_{II}^2 \left(4 \sin^2 \vartheta \cos \vartheta + \frac{\cos^2 2\vartheta}{\cos \vartheta} \right) + \Delta K_I \Delta K_{II} \sin \vartheta \left(2 \cos 2\vartheta - 4 \cos^2 \vartheta \right)} \quad (13)$$

Crack Propagation Criteria for Mixed Mode
The kinked pattern of a crack embedded in the microstress field above described can be analysed by adopting a mixed-mode crack propagation criterion. Several criteria for both stable and unstable crack propagation have been proposed for different materials. According to the *MTS-criterion* (Maximum Tensile Stress) by Erdogan and Sih [2, 3], the crack grows in the direction normal to the maximum principal stress (σ_α) direction or, equivalently, parallel to the maximum tangential stress:

$$\frac{\partial \sigma_\alpha}{\partial \alpha} = 0, \quad \frac{\partial^2 \sigma_\alpha}{\partial \alpha^2} < 0 \quad (14)$$

where the polar coordinate α is used to identify the position vector with respect to the crack tip direction (Fig. 4b). Others criteria have been proposed: for instance, the *zero shear stress criterion* by Maiti et al. [10], the *M-criterion* by Kong et al. [11] (based on the maximum stress triaxiality ratio $M = \sigma_H / \sigma_{eq}$, where σ_H is the hydrostatic stress and σ_{eq} is an equivalent stress such as the Von Mises stress), the maximum dilatational strain energy density criterion (*T-criterion,* Theocaris et al. [12]).

From experimental tests, it has been observed that the crack propagation direction usually tends to follow the local or global minimum extension of the plastic core region, i.e. the crack tends to reach the elastic region of the material outside the plastic zone developed around the crack tip. On this basis, the crack is assumed to follow the "easiest" path to reach the elastic region, that is, it tends to choose the shortest path from the crack tip to the elastic material outside the plastic zone. This path corresponds to the minimum plastic work needed to create a new portion of crack area. The so-called *R-criterion* (Shafique et al. [4, 5]) accomplishes such a hypothesis and can be written as follows:

$$\frac{\partial R_p}{\partial \alpha} = 0, \quad \frac{\partial^2 R_p}{\partial \alpha^2} > 0 \quad (15)$$

where R_p is the function which defines the radial distance from the crack tip to a generic point of the plastic zone boundary $F(I_1, J_2) = 0$ (I_1, J_2 are first invariant of stress tensor and second invariant of deviatoric stress tensor, respectively).

Short Crack Example
Some of the above described models for the assessment of the crack propagation at the microscale and the evaluation of the mean weighted SIF is herein applied to a carbon steel D6ac whose composition and mechanical parameters are presented in Tab. 1.

Tab. 1. Physical and mechanical parameters of the main elements in a carbon steel D6ac

	Element	volume fraction η [%]	Mass density ρ [kg/m³]	Young modulus E [Gpa]	Poisson's ratio v	Thermal expansion coeff. α [K¹]
Iron	Fe	~ 98.00	7870	200	0.29	1.20E-05

		~ 1.05	10220	330	0.38	5.35E-06
Molibden	Mb	~ 1.05	10220	330	0.38	5.35E-06
Cromium	Cr	~ 1.05	7190	248	0.30	6.20E-06

Tab. 2. Mean physical and mechanical parameters of the base material and the equivalent inclusion for the carbon steel D6ac

	Element	volume fraction η [%]	Mass density ρ [kg/m³]	Young modulus E [GPa]	Poisson's ratio ν	Thermal expansion coeff. α [K⁻¹]
Base material	Fe	~ 98.00	7870	200	0.29	1.20E-05
Equivalent inclusion	--	~ 2.10	8705	289	0.34	5.78E-06
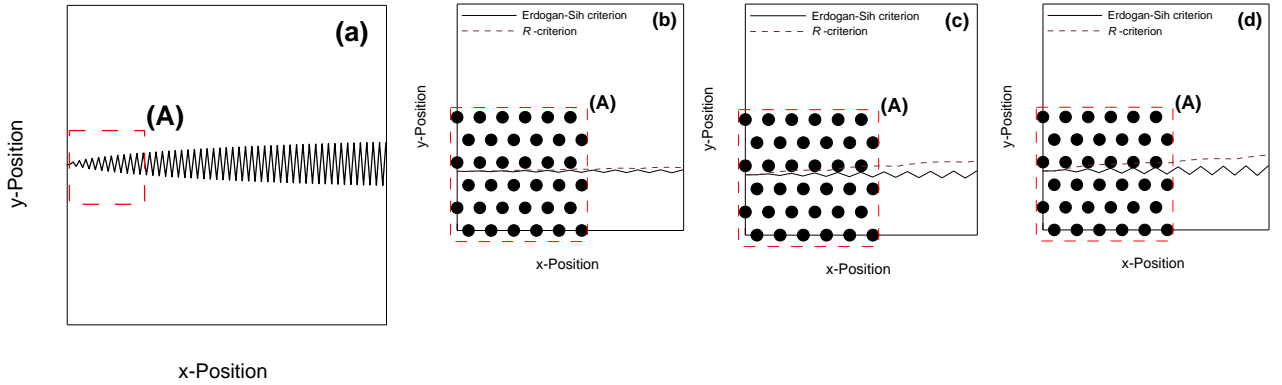
Fig. 6. (a) Path of an initially straight crack developing between two lines of inclusions in an infinite plate under remote uniform tensile stress σ_{0y}. Detail of the crack path at the microscale for (b) e/h= 1/2, (c) e/h=1/4, (d) e/h=1/5 (the distribution of inclusions is shown).

The mean weighted values of the physical and mechanical parameters of the secondary constituents, reduced to a single equivalent inclusion, are reported in Tab. 2.

The case of an initially cracked infinite plate under remote uniform tension σ_{0y}, with a straight crack normal to the applied stress, is herein examined. By using the equivalent inclusion volume fraction (Tab. 2) and considering an average inclusion diameter equal to about $20\mu m$ (e.g. see Ref. [13]), an inclusion spacing $d = h$ equal to about $234\mu m$ can be computed for a regular hexagonal distribution of inclusions (Fig. 2). The static crack extension is determined by applying the above described Erdogan-Sih criterion and the R-criterion and using the mixed mode SIFs based on the remote stress σ_{0y} (the local fluctuation of the stress component σ_y is negligible, as is shown in Fig. 3) and the shear microstress fluctuations $\tilde{\tau}$. In Fig. 6, the crack paths estimated for an initially straight crack located at $e/h = 1/2$ (Fig. 6b, $|\tilde{\tau}_a|/\sigma_{y0} \cong 0.0026$), $e/h = 1/4$ (Fig. 6c, $|\tilde{\tau}_a|/\sigma_{y0} \cong 0.0059$) and $e/h = 1/5$ (Fig. 6d, $|\tilde{\tau}_a|/\sigma_{y0} \cong 0.0085$) are plotted. The crack paths evaluated by such two criteria are similar, but the R-criterion produces a slight crack path deviation since the plastic zone shape is influenced in a complex way by the Mode I and Mode II SIFs which continuously change during the whole process of crack propagation.

Figure 7 shows the mean weighted equivalent SIF $\overline{K}_{I,eq}$ (see Eq. 12) against the dimensionless projected crack length l/d, for different position of the nominal horizontal crack line with respect to the inclusion arrangement. It can be observed that each curve tends to the slope 1/2 for long

cracks as in the case of a smooth straight crack, whereas such a ratio decreases for short cracks. In other words, the equivalent SIF can be written as $\overline{K}_{I,eq} = C \cdot l^{w/2}$, with $w<1$ for $l/d \cong 1$ and $w \to 1$ for high values of the l/d ratio.
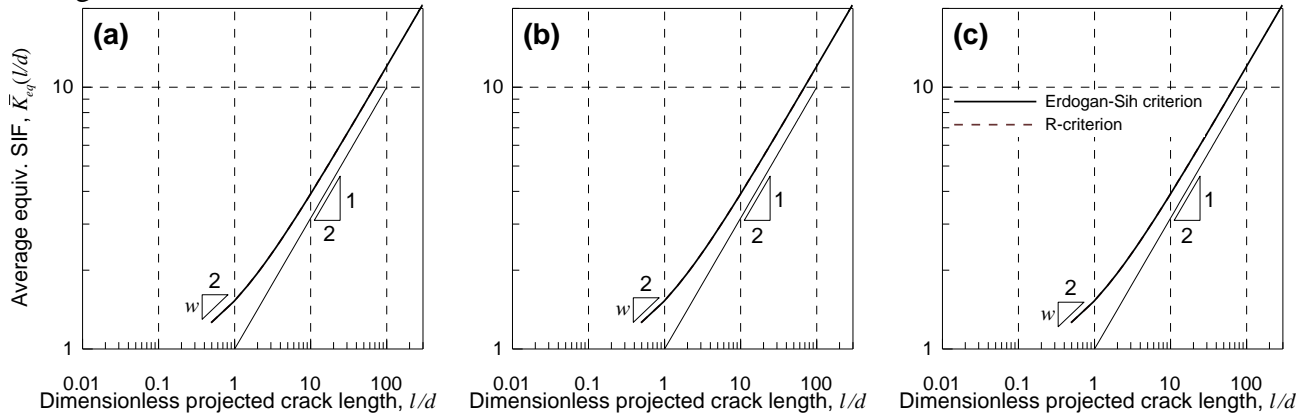
Fig. 7. Equivalent weighted average SIF for a nominally Mode I crack located at (a) $e/h=1/2$, (b) $e/h=1/4$, and (c) $e/h=1/5$.

Conclusions

In the present paper, a simple analytical model to assess the microstress variation due to material inhomogeneities and the corresponding trajectory of a propagating crack is proposed. In the case of metals, the inhomogeneities are treated by considering a two-phase material with an equivalent mean inclusion (characterized by a regular spatial distribution) responsible for a multiaxial fluctuating stress field which determines a mixed-mode crack propagation.

By adopting different mixed-mode crack growth criteria, the crack path can be deduced to depend on the main features of the material microstructure, here accounted in terms of an appropriate microstress field. It is shown that both the maximum principal stress criterion and the R-criterion (based on the minimum extension of the core plastic zone) evaluate a zig-zag crack pattern, characterised by a length scale related to both the volume fraction of inclusions and their mean size. A strong dependence of the crack path on the material microstructure is observed in the short crack regime. Moreover, by introducing a mean weighted equivalent SIF, the exponent of the equivalent SIF against crack length curves is shown to be smaller than 1/2, for crack lengths comparable with the inclusion spacing in the base material.

References

[1]   S. Suresh: *Metallurgical Trans* 14A (1985), p. 2375–2385.
[2]   F. Erdogan, G.C. Sih: J Basic Engng 85 (1963), p. 519–527.
[3]   G.C. Sih: Int. J. Fract 10 (1974), p. 305-321.
[4]   M.A.K. Shafique, K.K. Marwan: Engng Fract Mech 67 (2000), p. 397–419.
[5]   M.A.K. Shafique, K.K. Marwan: Int. J Plasticity 20 (2004), p. 55–84.
[6]   Ye.Ye. Deryugin, G.V. Lasko, S. Schmauder : http://www.ndt.net/article/cdcm2006/papers/lasko.pdf
[7]   A. Carpinteri, A. Spagnoli, S. Vantadori: 13th Int. Congress on Mesomech. (Mesomechanics 2011), 6-8 July 2011, Vicenza (Italy).
[8]   H. Kitagawa, R.Yuuki, T. Ohira: Engng Fract Mechs 7 (1975), p. 515–529.
[9]   YZ. Chen: Theor. Appl. Fract Mech 31 (1999), p. 223–232.
[10] S.K. Maiti, R.A. Smith: Int J Fract 23 (1983), p. 281–295.
[11] X.M. Kong, M. Schulter, W. Dahl: Engng Fract. Mech. 52 (1995), p. 379–388.

[12] P.S. Theocaris, G.A. Kardomateas, NP. Adrianopoulos: Engng Fract. Mech 17(1982), p.439-447.

[13] Y. Murakami. *Metal Fatigue: Effects of Small Defects and Nonmetallilc Inclusions*. Elsevier, Amsterdam (2002).